crystals

MDPI

Article

Synthesis and Characterization of Zinc Oxide Nanoparticle Anchored Carbon as Hybrid Adsorbent Materials for Effective Heavy Metals Uptake from Wastewater

Abdullah G. Alanazi, Mohamed A. Habila *, Zeid A. ALOthman and Ahmed-Yacine Badjah-Hadj-Ahmed

Chemistry Department, College of Science, King Saud University, Riyadh 11451, Saudi Arabia; zaothman@ksu.edu.sa (Z.A.A.)
* Correspondence: mhabila@ksu.edu.sa; Tel.: +966-1-4674-198; Fax: +966-1-4675-992

Abstract: Hybrid material-derived adsorbents have shown a great applicable efficiency in various fields, including industrial uses and environmental remediation. Herein, zinc oxide nanoparticle modified with carbon (ZnO-C) was fabricated and utilized for wastewater treatment through the adsorption of Zn(II), Cd(II), Co(II), and Mn(II). The surface and structural characteristics were examined using TEM, SEM, XRD, FTIR spectroscopy, EDS, and the BET surface area. Kinetics and equilibrium investigations were applied to optimize the adsorptive removal of Zn(II), Cd(II), Co(II), and Mn(II) onto ZnO-C. The results indicated that the formation of ZnO-C in crystalline sphere-like granules with a nano-size between 16 and 68 nm together with carbon matrix. In addition, the spherical granules of zinc oxide were gathered to form clusters. FTIR spectroscopy indicated that the ZnO-C surface was rich with OH groups and ZnO. The adsorption capacity 215, 213, 206, and 231 mg/g for Zn(II), Cd(II), Co(II), and Mn(II), respectively, at the optimal conditions pH between 5 and 6, a contact time of 180 min, and an adsorbent dose of 0.1 g/L. The adsorptive removal data modeling for the uptake of Zn(II), Cd(II), Co(II), and Mn(II) onto ZnO-C showed agreement with the assumption of the pseudo-second-order kinetic model and the Freundlich isotherm, suggesting a fast adsorption rate and a multilayered mechanism. The achieved adsorption capacity using the prepared ZnO-C was more effective compared to ZnO, carbon, Fe_3O_4, and Fe_3O_4-C. Real wastewater samples were applied, including valley water, industrial wastewater, and rain wastewater, and evaluated for the applicable uptake of Zn(II), Cd(II), Co(II), and Mn(II) using ZnO-C and Fe_3O_4-C with effective removal efficiency.

Keywords: zinc oxide nanoparticles; carbon; iron (III) oxide nanoparticles; adsorption; wastewater; kinetic and equilibrium studies

check for updates

Citation: Alanazi, A.G.; Habila, M.A.; ALOthman, Z.A.; Badjah-Hadj-Ahmed, A.-Y. Synthesis and Characterization of Zinc Oxide Nanoparticle Anchored Carbon as Hybrid Adsorbent Materials for Effective Heavy Metals Uptake from Wastewater. *Crystals* **2024**, *14*, 447. https://doi.org/10.3390/cryst14050447

Academic Editor: Nabeen K. Shrestha

Received: 14 March 2024
Revised: 29 April 2024
Accepted: 1 May 2024
Published: 8 May 2024

1. Introduction

Heavy metal polluted effluents originate from industrial activities and are a serious environmental hazard [1]. Heavy metals such as manganese, cadmium, cobalt, and zinc are naturally occurring elements. Small amounts of these elements are common in our environment, and they are actually necessary for our health. But large amounts of any of them may cause acute or chronic toxicity [2]. Heavy metals in the human body tend to bioaccumulate, which may result in damaged or reduced mental or central nervous function and damage to the blood composition, lungs, kidneys, or liver. For example, cobalt, one of the common toxic metals affecting the environment, is present in the wastewater of nuclear power plants and many other industries, such as the mining, metallurgical, electroplating, paint, pigment, and electronic industries [3]. High levels of cobalt may cause several health troubles, such as paralysis, diarrhea, low blood pressure, lung irritation, and bone defects [4]. Manganese, a naturally occurring metallic element, may contaminate groundwater as a result of weathering and the leaching of manganese-bearing rocks into

aquifers. Aquifers in certain regions of Quebec, other portions of Canada, and other countries (including Sweden, Vietnam, Bangladesh, Morocco, and others) contain naturally high quantities of manganese [5,6]. Although manganese is a vital trace element, it may be a strong neurotoxin in excess. The amount of manganese in drinking water is not regulated in the United States or Canada, since it is mostly seen as an aesthetic problem. Manganese concentrations greater than 100 g/L encourage the discoloration of laundry and hygienic items and provide an unpleasant flavor to drinks [7]. Zinc is extensively present in environmental components, including food and water [8,9]. Zinc has a maximum recommended value of 5.00 mg/L in drinking water, according to the European Commission Drinking Water Directive, the World Health Organization and its Guidelines for Drinking Water Quality, and the US Environmental Protection Agency (EPA). An over-dose exposure to zinc leads to immediate symptoms, such as vomiting, nausea, and anemia [10]. Cadmium is one of the most harmful non-essential heavy metals in the environment, and it comes from many sources, including wastewater from the metal plating, nickel–cadmium battery, phosphate fertilizer, mining, pigment, stabilizer, alloy, petroleum refining, welding, and pulp industries, as these industries produce elevated levels of cadmium ions. Cadmium toxicity results in kidney damage, cancer, and lung dysfunction [11]. The maximum recommended value of cadmium in drinking water is 0.005 mg/L [12]. Therefore, many research investigations have been conducted to develop tools for wastewater purification. The removal of heavy metal pollutants from water can be achieved using many methods, including chemical precipitation, flotation, biosorption, electrolytic recovery, membrane separation, and removal through adsorption onto minerals or activated carbon [13–16]. Usually, these methods are restricted by many factors, such as their processing efficiency, operational method, energy requirements, and economic benefit. Adsorption is an effective, straightforward, and affordable technique for removing heavy metals from water [17,18]. An effective sorbent should have a high heavy metal sorption capacity and a low cost, and should be renewable and durable [19]. Although they are costly and ineffective for treating water, carbon materials are reported as efficient adsorbents for heavy metals [20,21]. Carbon-incorporated materials are durable and possess physicochemical stability, which enhances wastewater treatment applications [22].

Recently, nanostructure-based materials have demonstrated higher efficiencies in wastewater treatment applications compared to traditional adsorbents [23,24]. Nanostructure adsorbents, such as manganese oxides, titanium oxides, iron oxides, and zinc oxides, have shown promising results in the removal of heavy metals. Zinc oxide is reported to be a proper adsorbent for organic and inorganic pollutants; however, the process suffers from many technical problems related to operation and efficiency [1,25–27]. Due to their outstanding optical, electrical, photonic, and microbiological capabilities, among others, zinc oxide (ZnO) nanoparticles are widely employed in many new multifunctional materials. Zinc oxide nanoparticle derived materials could be utilized in various manufacturing sectors, such as those that manufacture rubber, plastics, cosmetics, pharmaceuticals, paints, soap, batteries, electrical equipment, optoelectronics, biomedical science equipment, etc.; the demand for zinc oxide is always rising [28,29]. In addition, zinc oxide nanoparticles have been investigated for water treatment by adsorption various heavy metal such as Cu(II), Cr(VI), Cd(II) and Pb(II) [30–33].

Hybrid materials, including carbon and metal oxide nanoparticles, have been reported as a novel category of materials with enhanced properties for catalysis, adsorption, precontraction, and medical applications [34,35]. Various methods have been applied to fabricate ZnO-derived hybrid adsorbent materials. For example, ultrasonic waves have been applied to enhance the formation of cellulose-modified zinc oxide nanoparticles from sawdust sources and investigate their capacity for methylene blue adsorption [36]. Liu et al. applied the solvothermal method to fabricate hydrostable cesium lead bromide–titania hybrid materials for the visible light photodegradation of tetracycline hydrochloride [37]. He et al. prepared Ti_3C_2/UiO-66-NH_2 using the in situ solvothermal process for the photocatalytic removal of Cr(VI) [38]. Nie et al. incorporated ZnO with Porous Carbon for

Adsorption of Methylene Blue [39]. The combination of metal oxides with carbon produces a hybrid material with superior properties compared to single-metal oxide or pure carbon. In addition, hybrid nano-adsorbent materials such as zinc oxide nanoparticles modified with graphene have shown an improved tendency to decompose organic pollutants [40]. Regeneration of adsorbent materials is necessary to assess sustainability and effectiveness of the wastewater treatment process. The possibility to control adsorption/desorption processes is characteristic for recyclable adsorbents, which enable saving the environment. Diluted acid solution such as nitric acid and hydrochloric acid, as well as EDTA solutions, are reported as effective eluents for regenerating adsorbent materials [41–43].

Research in this field is still ongoing, with the aim of improving the efficiency of nanocomposites in the removal of pollutants, even through adsorption or photocatalytic degradation. The novelty of this work is to combine carbon structure with ZnO nanoparticles to produce an efficient extractor of pollutants from wastewater. Thus, this work aimed to fabricate zinc oxide-anchored carbon (ZnO-C) as a hybrid adsorbent to enhance the adsorption capacity for heavy metal uptake. In addition, the produced ZnO-C was characterized using SEM, TEM, XRD, the surface area, and EDS. Furthermore, the achieved adsorption capacity was compared with that of other adsorbents, including zinc oxide, carbon, and Fe_3O_4-C. Moreover, wastewater samples were purified using the developed ZnO-C hybrid adsorbent materials.

2. Experimental Section

2.1. Materials

The materials, including analytical-grade zinc acetate, polyethylene glycol, sodium hydroxide, zinc oxide, hydrochloric acid, zinc nitrate, cobalt nitrate, cadmium nitrate, and manganese nitrate, were purchased from Sigma, USA. Carbon and Fe_3O_4-C were obtained from our laboratory, prepared according to our previously published work by Habila et al. [44].

2.2. Fabrication of Zinc Oxide Nanoparticle Anchored Carbon (ZnO-C)

For preparation of zinc oxide nanoparticle anchored carbon (ZnO-C), 21 g of zinc acetate, 10 g of polyethylene glycol, and 10 g of carbon were well mixed in a 1:2 ethanol/water medium; then, 100 mL of NaOH (0.1 M) was added to the mixture, and it was stirred for an hour. After that, the mixture was kept in an oven at 110 °C for 17 h. The formed precipitate was then isolated using centrifugation and treated in a muffle furnace at 750 °C for one hour, in inert nitrogen atmosphere. The obtained ZnO-C was ground in a mortar and washed several times with ethanol and water, and then dried in an oven at 105 °C for 10 h. The produced ZnO-C was characterized using TEM, SEM, FTIR, XRD, EDS, and the surface area as explained in the Supplementary Materials.

2.3. Optimization of Adsorptive Removal of Zn(II), Cd(II), Co(II), and Mn(II) for Wastewater Purification

A total of 0.02 g of the metal oxide nanoparticles, ZnO, Fe_3O_4, or their derived carbon hybrid materials (ZnO-C or Fe_3O_4-C), was mixed with 20 mL of a mixed heavy metal solution that included Zn(II), Cd(II), Co(II), and Mn(II). Then, the pH was optimized using a phosphate buffer. The mixture was shaken at room temperature for 180 min. Then, the aqueous solution was separated using centrifugation. The change in the heavy metal ion concentration was determined using ICP-MS. The adsorptive removal capacity was evaluated using Equation (1):

$$q_e = \frac{(C_0 - C_e) \times V}{M} \quad (1)$$

where q_e is the adsorptive removal capacity (mg/g) for Zn(II), Cd(II), Co(II), or Mn(II) onto the metal oxide nanoparticles, ZnO, Fe_3O_4, or their derived carbon hybrid materials (ZnO-C or Fe_3O_4-C).

C_0 is the initial concentration of Zn(II), Cd(II), Co(II), or Mn(II).

C_f is the final concentration of Zn(II), Cd(II), Co(II), or Mn(II) after adsorption.

V is the volume of the solution of the whole adsorption mixture.

M is the mass of the metal oxide nanoparticles, ZnO, Fe_3O_4, or their derived carbon hybrid materials (ZnO-C or Fe_3O_4-C).

The previously described steps for adsorptive removal were operated several times to assess the effects of the pH of the adsorption medium in the range 2–7, the time of contact in the range 5–1200 min, the dose of ZnO-C in the range 0.1–0.6 g/L, and the concentration of Zn(II), Cd(II), Co(II), and Mn(II) in the range 25–300 mg/L. Kinetic models and equilibrium isotherms were applied to investigate the adsorption rate and predict the adsorption behavior. In addition, wastewater samples were collected from Saudi Arabia, filtered, and used to evaluate the adsorption under optimized conditions for the uptake of Zn(II), Cd(II), Co(II), and Mn(II) onto ZnO-C or Fe_3O_4-C.

For regeneration of the ZnO-C after each desorption cycle, 10 mL of Na_2EDTA (0.01 M) was added and the mixture was exposed for ultrasonic waves for 30 s, followed by shaking (150 rpm) for 60 min. The regenerated ZnO-C was then separated by centrifuge and washed with deionized water and dried in an oven at 110 for 10 h, then subjected for the next use. The recycling efficiency was calculated as a ratio based on the first application cycle from Equation (2) [45].

$$RE_x\% = \left(\frac{q_x}{q_{1st}}\right) \times 100 \quad (2)$$

where $RE_x\%$ is the recyclable efficiency of cycle x, q_x is the adsorption capacity for heavy metals uptake using ZnO-C of cycle number x, and q_{1st} is the adsorption capacity for heavy metals uptake using ZnO-C of the first cycle (x = 1).

3. Results and Discussion

3.1. Characteristics of the Developed ZnO-C Hybrid Adsorbent Materials

The morphology of the fabricated ZnO-C hybrid adsorbent materials was described using SEM/EDS (Figure 1A–C) which revealed a sphere-like granulated structure of the formed ZnO-C hybrid materials in the nanoscale size range of 16–68 nm. In addition, clusters are formed from the aggregation of the spherical granules. In addition, the SEM image (Figure 1A) showed pores between the aggregated zinc oxide nanoparticles. A similar particles shape is reported by Fouladi-Fard et al. for the preparation of a ZnO nanoparticle by solvothermal process. The formed ZnO structures exhibited an oval and spherical-like structure with a particle size in the range 55–70 nm [46]. The TEM showed that the ZnO nanoparticles are embedded in carbon matrix indicating the formation of ZnO-C hybrid materials (Figure 2A–D). The ZnO nanoparticles are formed with particle size about 10–20 nm, in addition to aggregated particles which are more than 300 nm (Figure 2A). In addition, the added TEM images (Figure 2C,D) showed porous carbon which is formed around the zinc oxide nanoparticles. The EDS analysis indicated the presence of Zn on the granules' surfaces, together with carbon and oxygen. The detected ratios were 13.64, 22.15, and 64.21 for C, O, and Zn, respectively.

The BET surface area was reported as 24.84 m^2/g. The total pore volume of pores was 0.097901 cm^3/g and the adsorption average pore diameter was 256.124 Å as indicated from adsorption/desorption nitrogen isotherm (Table 1). The surface area reported in this work is slightly lower than that reported by Al-Rawashdeh et al., whose reported BET surface area for graphene oxide-anchored zinc oxide nanoparticles (GO–ZnO) as 36.95 m^2/g [47]. In addition, Gu et al. prepared ZnO nanoparticles for the removal of Cr(III) and reported a BET surface area of 26.7 m^2/g [32].

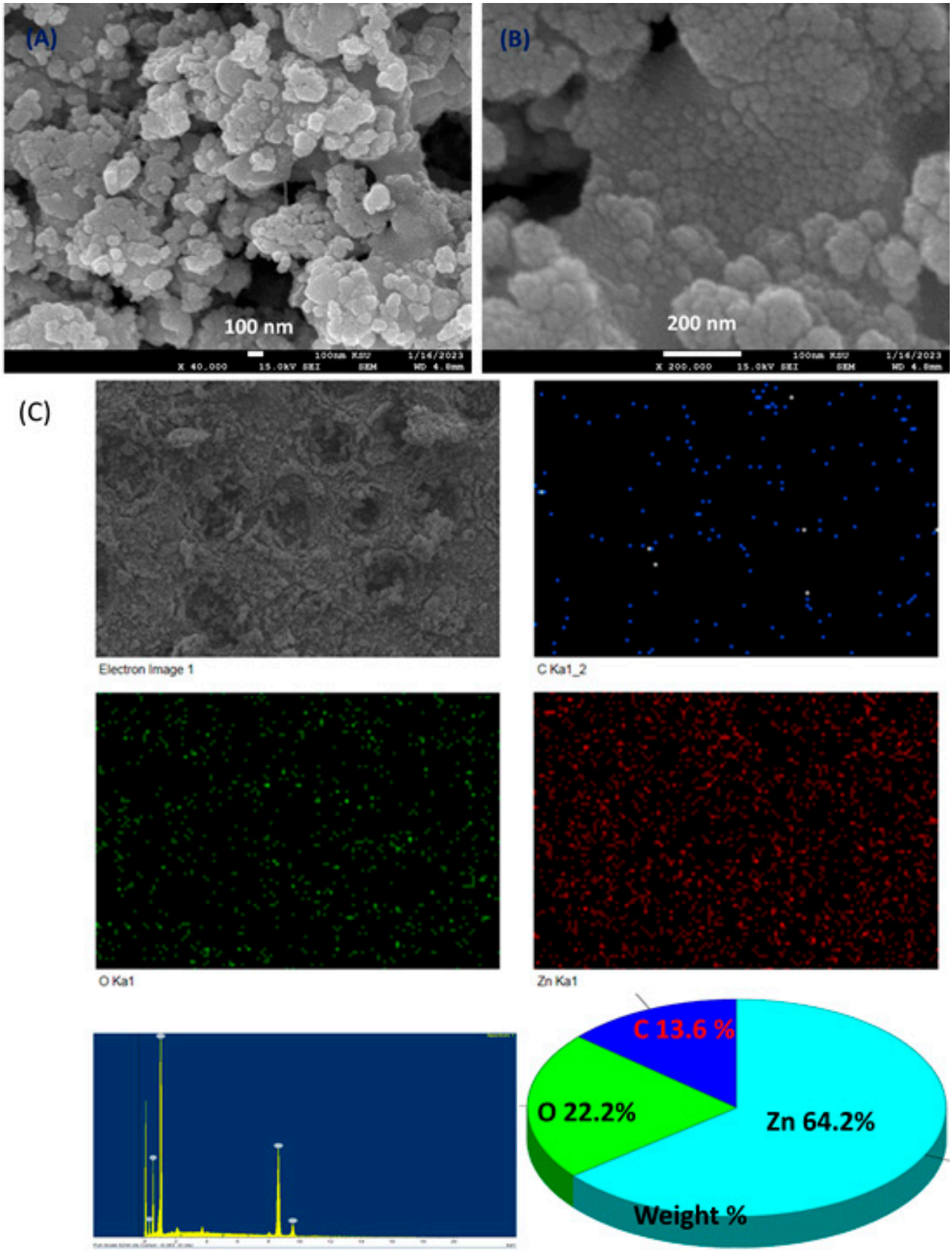

Figure 1. SEM/EDS mapping characterization of ZnO-C. (**A**) low magnification SEM (**B**) high magnification SEM (**C**) EDS mapping.

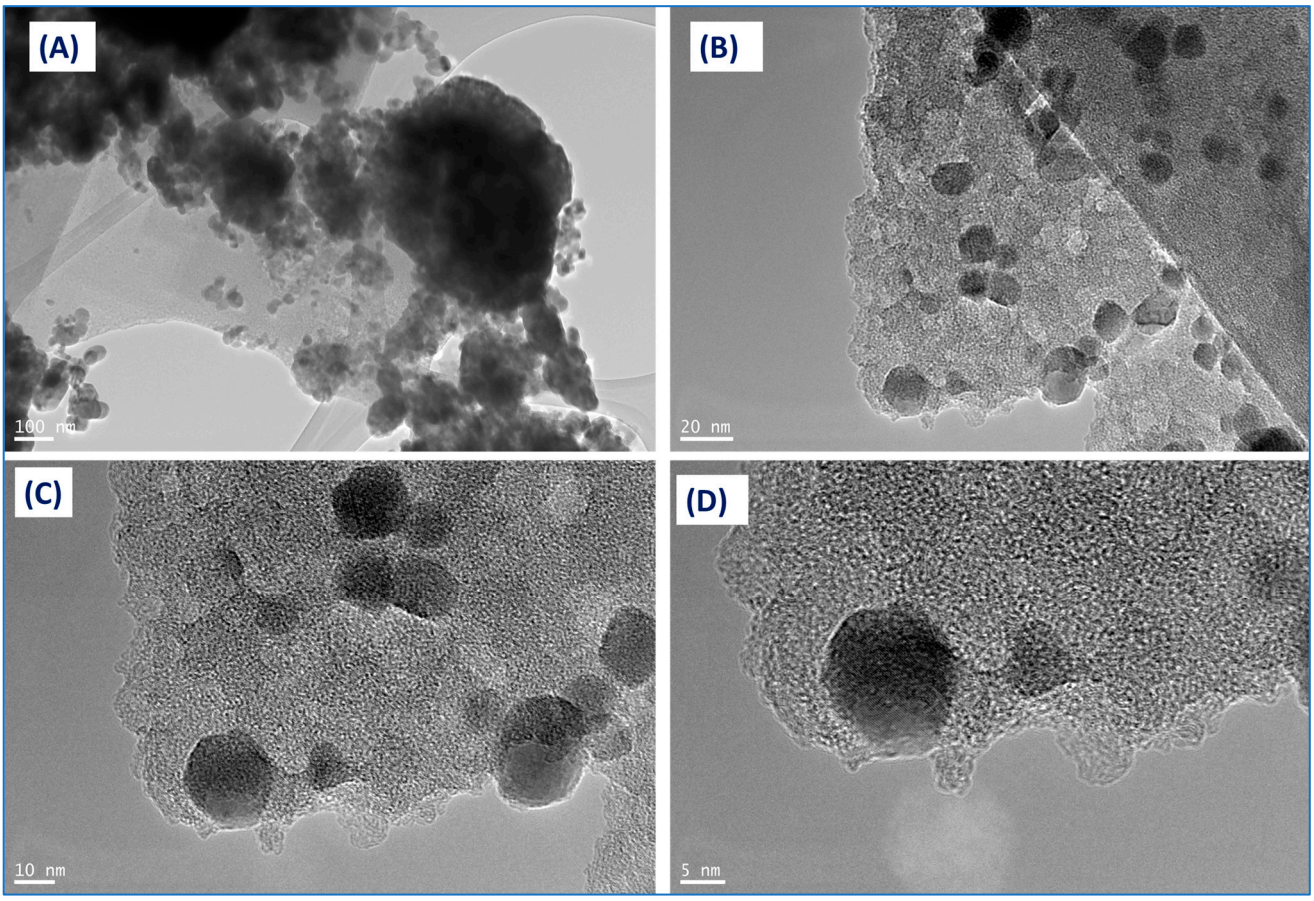

Figure 2. TEM characterization of ZnO-C at various scales (**A**) 100 nm (**B**) 20 nm (**C**) 10 nm (**D**) 5 nm.

Table 1. Correlation between surface area and adsorption capacity for ZnO, Fe_3O_4, carbon, ZnO-C, and Fe_3O_4-C.

	BET Surface Area (m^2/g)	Total Pore Volume of Pores (cm^3/g)	Adsorption Average Pore Diameter (Å)	Adsorption Capacity (mg/g)			
				Mn(II)	Co(II)	Cd(II)	Zn(II)
ZnO	16.8	0.080823	189.794	111	85	116	101
Fe_3O_4	14.2	0.070926	242.769	83	116	103	125
C	163.8	0.161620	94.187	90	106	91	100
ZnO-C	24.8	0.097901	256.124	196	173	180	189
Fe_3O_4-C	19.6	0.147731	316.588	167	165	173	177

The developed ZnO-C was characterized using FTIR spectroscopy (Figure 3e), which indicated main peaks between 3300 and 3700 cm^{-1} due to the stretching vibration of the O-H groups. The peaks around 2900 cm^{-1} were attributed to the aliphatic C-H, while the peak at around 1600 cm^{-1} was due to carbonyl groups (C=O). The peak between 1400 and 1500 was attributed to O-H binding. The peak between 400 and 470 cm^{-1} was attributed to the stretching vibration of the Zn-O bond. For comparison, the FTIR spectra for other adsorbents are provided in Figure 3 ((a) carbon, (b) Fe_3O_4, (c) Fe_3O_4-C, and (d) ZnO). Hydroxyl groups are detected in all adsorbent's samples, while carbonyl groups are detected in case of (b) Fe_3O_4, (c) Fe_3O_4-C, and (d) ZnO. In addition, Fe-O is detected in case of (b) Fe_3O_4, and (c) Fe_3O_4-C. An Aliphatic C-H group is detected in case of Fe_3O_4 at about 2900 cm^{-1} due because the Fe_3O_4 nanoparticles were previously prepared with citrate stabilization [45]. The surface functional groups play an important role in the adsorption process for the uptake of heavy metals.

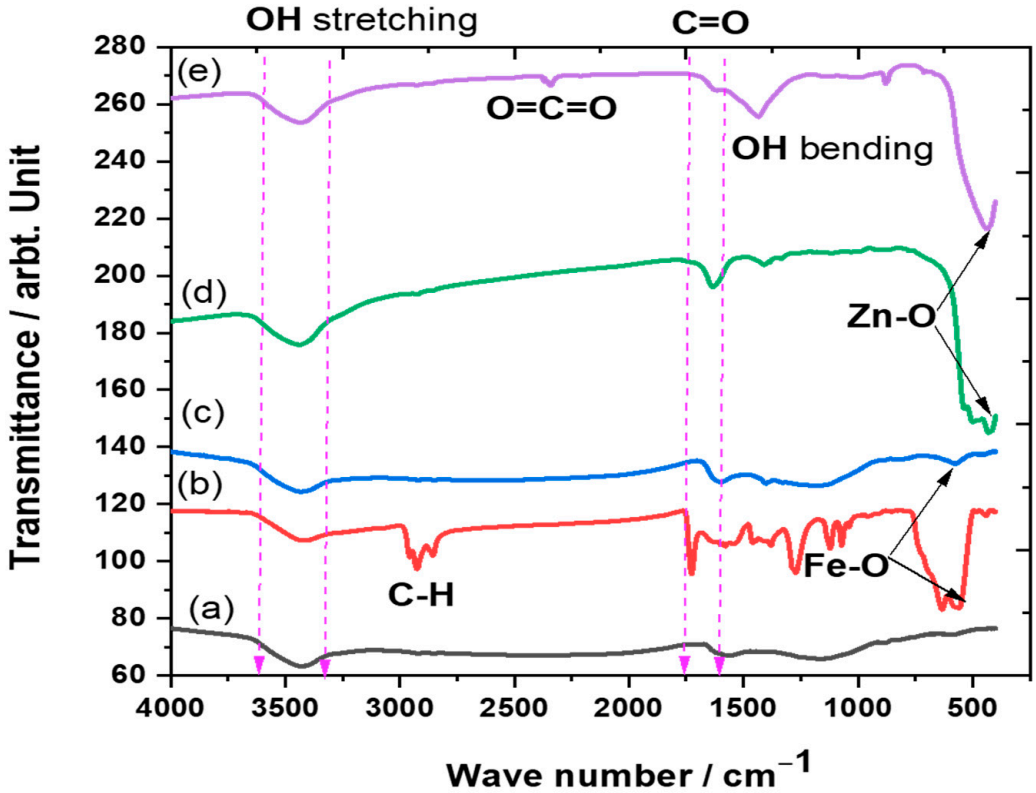

Figure 3. FTIR spectra of (**a**) carbon, (**b**) Fe_3O_4, (**c**) Fe_3O_4-C, (**d**) ZnO, and (**e**) ZnO-C.

The XRD analysis (Figure 4A,B) compared the peaks related to pure zinc oxide and zinc oxide anchored carbon hybrid materials (ZnO-C). The pure zinc oxide showed peaks at 2θ of 31.7° (100), 34.4° (002), 36.2° (101), 47.6° (102), 56.6° (110), 62.9° (103), and 67.1° (112) according to the Joint Committee on Powder Diffraction Standards (JCPDS No. 89-1397) [48], whereas ZnO-C exhibited similar peaks with missing of the peak at 2θ of 67.1° (112), which may be attributed to carbon shielding. In addition, the peaks of ZnO in the ZnO-C adsorbent are shifted, and the peaks' intensity is reduced due to incorporation of ZnO with carbon and ZnO aggregation into larger particles as present in TEM (Figure 2). These reasons lead to the change in the intensities of the main ZnO reflections (100, 002, 101). The shift in the peaks' location due to doping are previously reported in El Aakib et al. for pure and aluminum-doped zinc oxide nanoparticles [49]. Furthermore, the C showed a lower intensity peak between 2θ of 17°–25° due to the carbon matrix in the ZnO-C hybrid adsorbent materials [50,51]. The successful fabrication of zinc oxide nanoparticle anchored carbon is expected to improve the application of the formed hybrid materials for the adsorption of heavy metals. Rodríguez et al. developed a zinc oxide/graphene nanocomposite and indicated that the removal efficiency of Al and Cu were 19.9 mg/g and 33.5 mg/g, respectively, owing to the fact that the coating of graphene with ZnO nanoparticles enhanced its adsorption capacity [52].

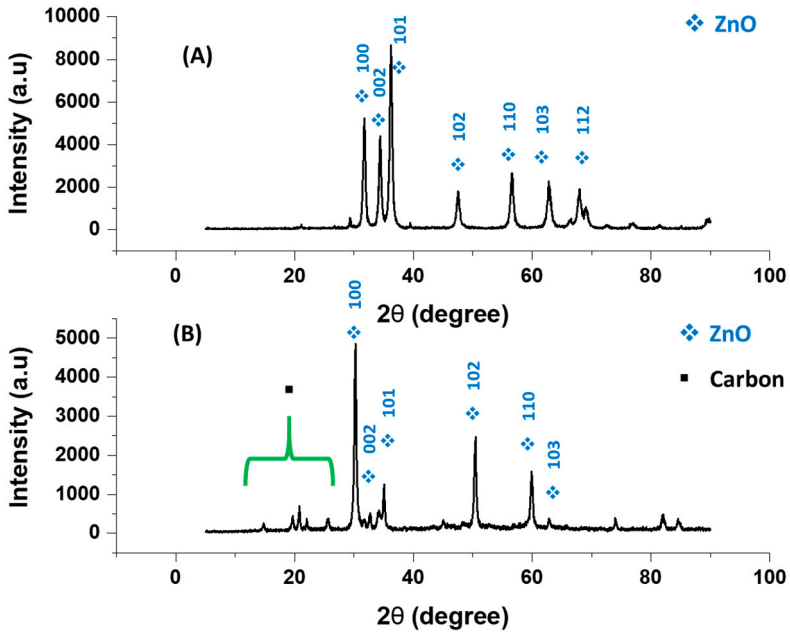

Figure 4. XRD spectra of (**A**) ZnO and (**B**) ZnO-C.

3.2. Utilization of Developed Hybrid Materials for Adsorption Applications

The metal oxide nanoparticles, including ZnO, Fe_3O_4, and their derived carbon hybrid materials (ZnO-C and Fe_3O_4-C), were evaluated for their ability to adsorb Zn(II), Cd(II), Co(II), and Mn(II) from an aqueous solution, as presented in Figure 5. The adsorption capacity of ZnO was 101, 116, 85, and 111 mg/g for Zn(II), Cd(II), Co(II), and Mn(II), respectively, while for Fe_3O_4 it was 125, 101.3, 116, and 83 mg/g for Zn(II), Cd(II), Co(II), and Mn(II), respectively. The adsorption capacity of carbon was 100, 91, 106, and 90 for Zn(II), Cd(II), Co(II), and Mn(II), respectively. On the other hand, the metal oxide-anchored carbon hybrid adsorbent materials exhibited a higher adsorption performance for the removal of heavy metals due to a synergic effect. In addition, the developed ZnO-C exhibited the highest adsorption capacity at 189, 180, 173, and 196 mg/g for Zn(II), Cd(II), Co(II), and Mn(II), respectively, compared to Fe_3O_4-C, which demonstrated an adsorption capacity of 177, 173, 165, and 167 mg/g for Zn(II), Cd(II), Co(II), and Mn(II), respectively. These results agree with the findings indicated by Hadadian et al., who reported that the combination of zinc oxide nanoparticles with graphene improved the adsorption capacity for nickel removal [53].

The variation in the adsorption of Zn(II), Cd(II), Co(II), and Mn(II) onto the tested adsorbents, including ZnO, Fe_3O_4, carbon, ZnO-C, and Fe_3O_4-C, can be attributed to the surface area and surface functional groups. The surface areas and pore volume are presented in Table 1. As the surface area of the metal oxide and metal oxide-derived carbon materials increased, the efficiency of the removal of heavy metals increased. In the case of the carbon adsorbent, the surface area and total pore volume of pores (0.161620 cm^3/g) were the highest, but the adsorption capacity and the adsorption average pore diameter (94.187 Å) were the lower than that of metal oxide-coated carbon, which may be attributed to the active surface site's nature and the characteristics of the present functional groups.

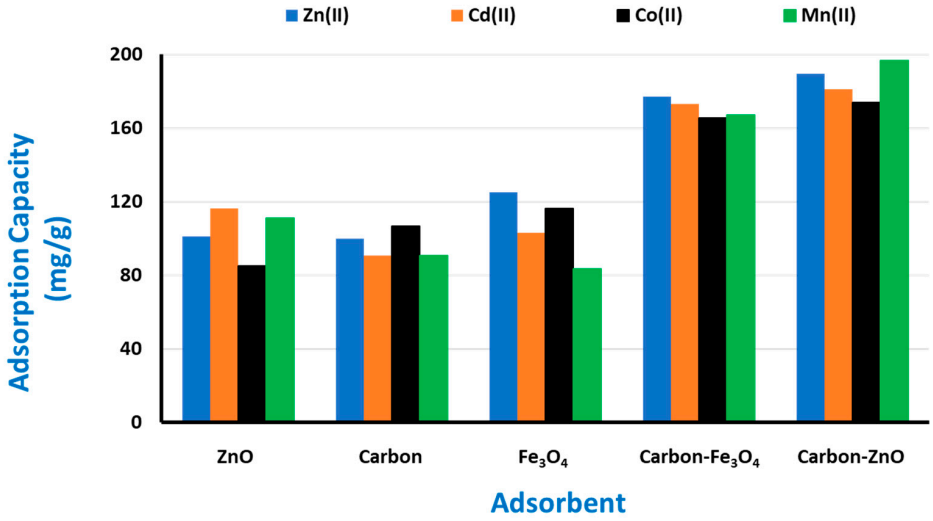

Figure 5. Investigation of the adsorption capacity of various adsorbents for the removal of Zn(II), Cd(II), Co(II), and Mn(II); pH: 6, time: 180 min, and adsorbent dose: 0.15 g/L.

3.3. Optimizing the Most Influencing Factors

The common effective factors influencing the adsorption efficiency during wastewater treatment were the pH, adsorbent dose, and time of contact. Therefore, various investigations were applied to optimize the adsorptive removal of Zn(II), Cd(II), Co(II), and Mn(II) using ZnO-C. The pH was studied in a range from 2 to 7 (Figure 6). The maximum adsorption capacity was achieved in an acidic medium with a pH between 5 and 6. These results agreed with previous adsorption methods using a ZnO-based adsorbent for the removal of Cu(II), which was conducted at a pH between 4 and 4.8 [54]. In addition, the pH was reported to be between 3 and 7 by Gu et al. for the adsorption of Cr(III) onto ZnO nanoparticles [33]. The mechanism of adsorption may include various driving forces, such as van der Waals, electrostatic, and dipole–dipole interactions between the heavy metal ions and the active sites on the ZnO-C surfaces, including OH groups. In the strongly acidic range, the protonation of the functional groups on the ZnO-C adsorbent surfaces as well as the competition between H^+ and heavy metal cations led to minimal adsorption capacities at pH 2.

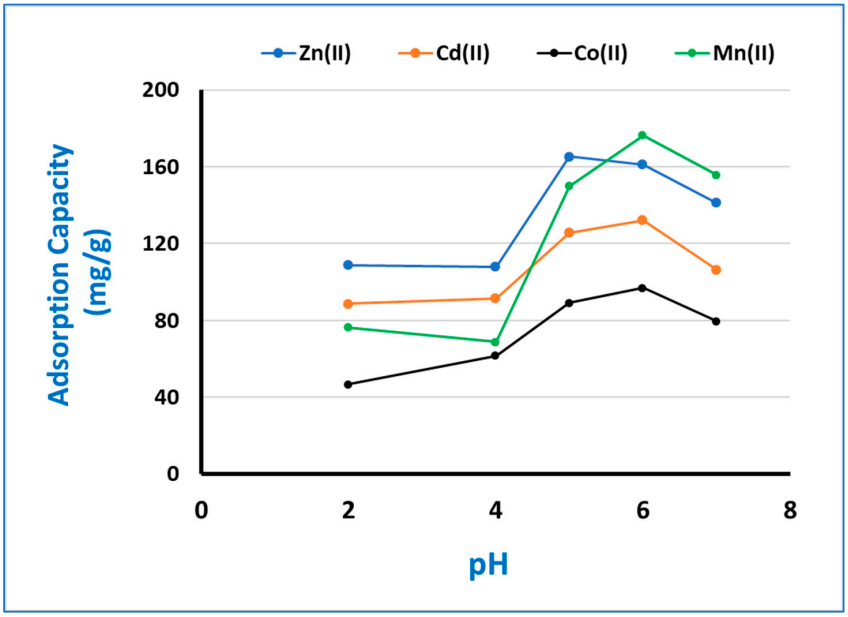

Figure 6. Influence of pH on the removal of Zn(II), Cd(II), Co(II), and Mn(II) using ZnO-C (time: 180 min and adsorbent dose: 0.15 g/L).

The ZnO-C adsorbent dose was investigated in the range of 0.1–0.6 g/L, and the related adsorption capacity is presented in Figure 7. The maximum adsorption capacity was reported at a dose of 0.1 g/L, with values of 215, 213, 206, and 231 mg/g for Zn(II), Cd(II), Co(II), and Mn(II), respectively. By increasing the ZnO-C dose, the adsorption capacity decreased. This could be attributed to an increase in unoccupied sites resulting from the increase in ZnO-C at a constant heavy metal ion concentration. A similar trend for the influence of dose on the adsorption capacity was previously reported by Habila et al. for the adsorption of arsenic and mercury onto CNT/SDS-alumina nanoparticles [55].

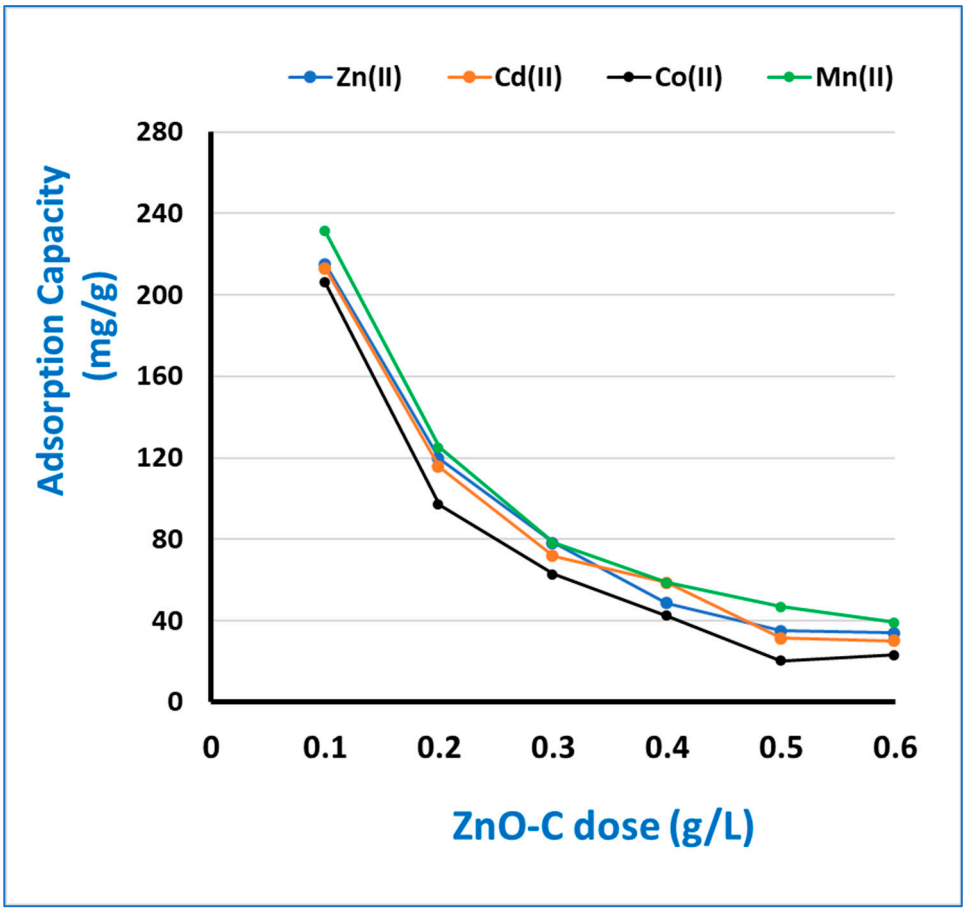

Figure 7. Influence of ZnO-C dose on the removal of Zn(II), Cd(II), Co(II), and Mn(II) using ZnO-C (pH: 6, time: 180 min).

Moreover, the influence of the contact time of Zn(II), Cd(II), Co(II), and Mn(II) with the ZnO-C was investigated in a range between 5 and 1200 min. By increasing the time from 5 to 180, a gradual improvement in the adsorption capacity was noticed (Figure 8). Approximately, at contact time of 180 min, the steady-stage equilibrium occurs, at which point the rate of adsorption was equal to the rate of the desorption processes. Herein, the reported equilibrium time of 180 min was considered a fast adsorption rate, which indicates the effectiveness of the prepared ZnO-C for the removal of Zn(II), Cd(II), Co(II), and Mn(II), with a capacity of 189, 180, 173, and 196 mg/L, respectively.

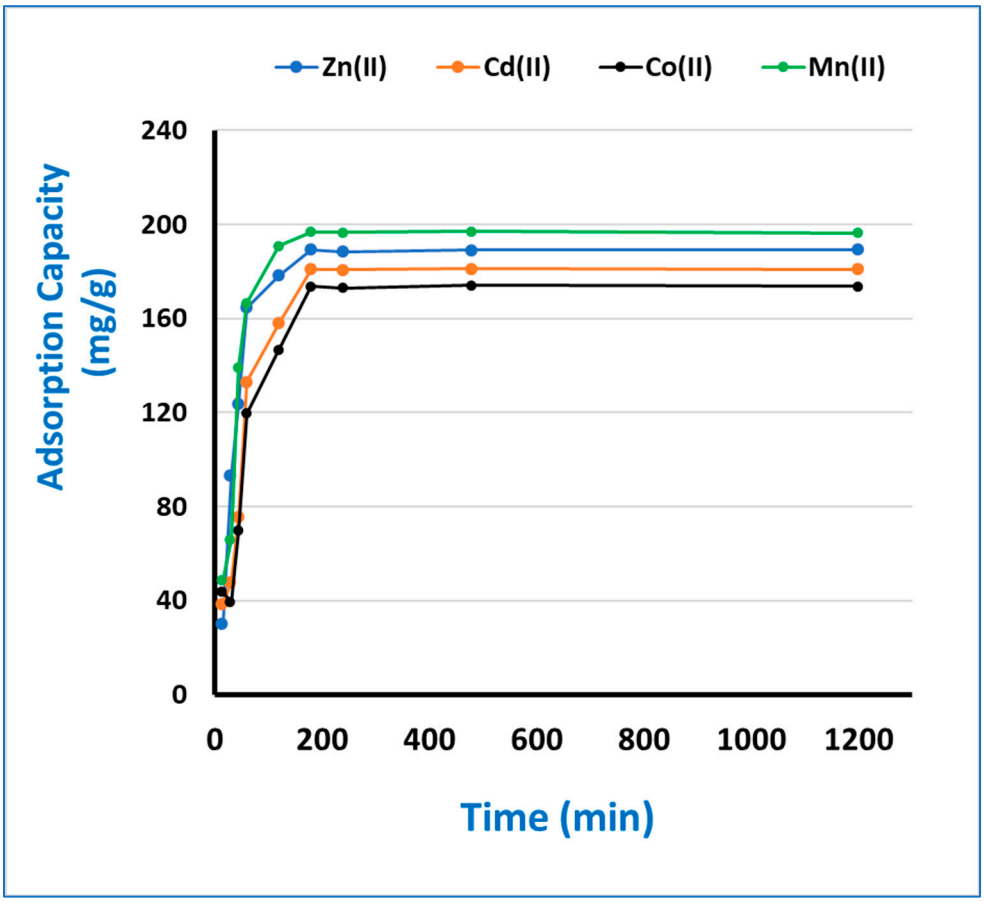

Figure 8. Influence of contact time on the removal of Zn(II), Cd(II), Co(II), and Mn(II) using ZnO-C (pH: 6 and adsorbent dose: 0.15 g/L).

3.4. Kinetic and Equilibrium Modeling

Applying adsorption theories is important for studying the characteristics of hybrid adsorbent materials to enhance their performance and develop a well-controlled process for wastewater treatments [55,56]. To deeply assess the interaction between the developed ZnO-C and Zn(II), Cd(II), Co(II), and Mn(II), various models were applied, such as the pseudo-first-order, pseudo-second-order, Langmuir isotherm, and Freundlich isotherm models, as stated in the related equations provided in Table 2.

Table 2. Kinetic and equilibrium equations for the applied pseudo-first-order, pseudo-second-order, Langmuir isotherm, and Freundlich isotherm models.

Model	Equation	Constants
Pseudo-1st-order model	$\log(qe - qt) = \log qe - \frac{K_1}{2.303}.t$	K_1: the rate constant of the pseudo-1st-order model (min^{-1}).
Pseudo-2nd-order model	$\frac{t}{qe} = \frac{1}{K_2(qe)^2} + \frac{1}{qe}.t$	K_2: the rate constant of the pseudo-2nd-order model (min^{-1}).
Langmuir isotherm model	$\frac{C_e}{q_e} = (\frac{1}{Q^0_{max}})\ C_e + \frac{1}{Q^0_{max}K_L}$	$Q^0{}_{max}$ (mg/g): maximum adsorption capacity. K_L (L/mg): a constant associated with the affinity of ZnO-C and the adsorbed heavy metal ions.
Freundlich isotherm model	$\log qe = \log K_F + \frac{1}{n}Ce$	K_F $(mg/g)/(mg/L)^n$: Freundlich constant. n (dimensionless): Freundlich intensity parameter.

The pseudo-first-order kinetic model (Figure 9) (Table 3) revealed a calculated adsorption capacity of 19.9, 233.1, 42.4, and 19.6 mg/g for Zn(II), Cd(II), Co(II), and Mn(II),

respectively, which significantly differed from the experimental capacity (189, 180, 173, and 196 mg/L for Zn(II), Cd(II), Co(II), and Mn(II), respectively). The pseudo-second-order kinetic model (Figure 10) (Table 3) revealed a calculated adsorption capacity of 196.1, 188.7, 181.8, and 200.0 mg/g for Zn(II), Cd(II), Co(II), and Mn(II), respectively, which was close to the experimental adsorption capacity (189, 180, 173, and 196 mg/L for Zn(II), Cd(II), Co(II), and Mn(II), respectively). Therefore, the pseudo-second-order model was the more suitable model for describing the adsorption process. These results indicate that the adsorption process onto the developed ZnO-C occurred over three steps: migration of Zn(II), Cd(II), Co(II), and Mn(II) in the adsorption solution; arrangement at the ZnO-C surfaces; and migration through the pores [57]. By applying the Langmuir isotherm plot (Figure 11) for the adsorption of Zn(II), Cd(II), Co(II), and Mn(II) onto ZnO-C, the calculated constant (Table 4) and the related correlation coefficient indicated that this model was not applicable for describing the adsorption process. When plotting the Freundlich isotherm (Figure 12), the calculated constants (Table 4) indicated a strong correlation, which confirmed the multilayer adsorption and heterogenous surfaces according to the Freundlich assumptions.

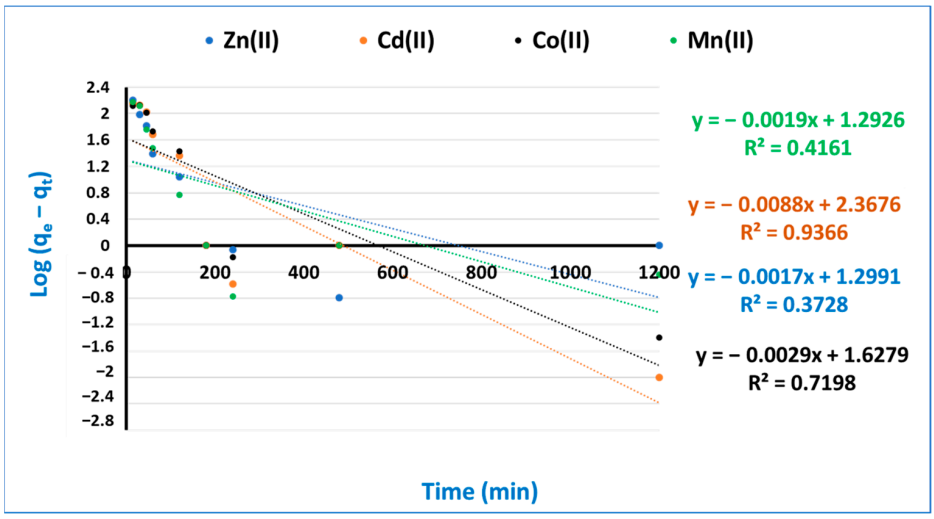

Figure 9. The pseudo-first-order plot for adsorption of Zn(II), Cd(II), Co(II), and Mn(II) onto ZnO-C (pH: 6 and adsorbent dose: 0.15 g/L).

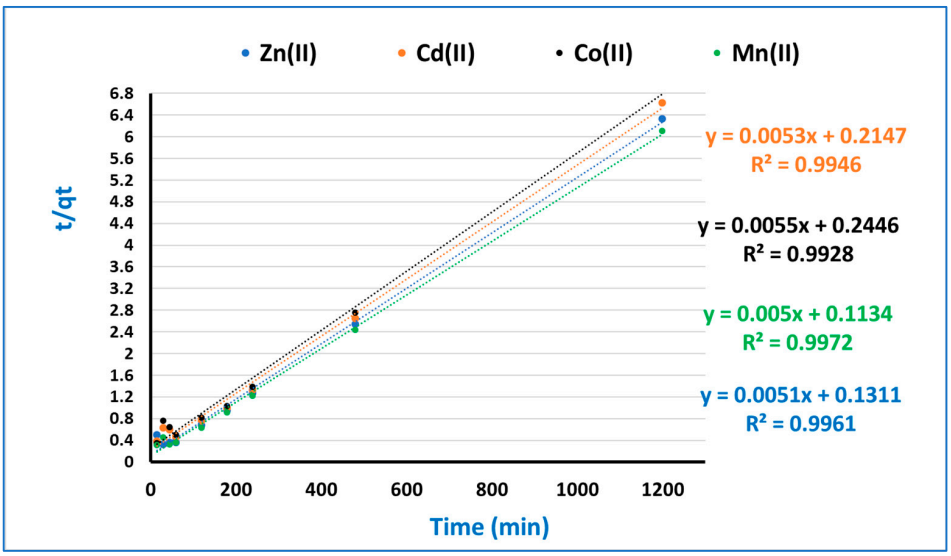

Figure 10. The pseudo-second-order plot for adsorption of Zn(II), Cd(II), Co(II), and Mn(II) onto ZnO-C (pH: 6 and adsorbent dose: 0.15 g/L).

Table 3. The pseudo-first-order and pseudo-second-order constants for adsorption of Zn(II), Cd(II), Co(II), and Mn(II) onto ZnO-C (pH: 6 and adsorbent dose: 0.15 g/L).

		Pseudo-First-Order			Pseudo-Second-Order		
	q_e,exp (mg/g)	K_1 (min^{-1})	q_e,cal (mg/g)	R^2	K_2 (g/mg·min)	q_e,cal (mg/g)	R^2
Zn(II)	183.0	0.000738	19.9	0.37	0.000198	196.1	0.99
Cd(II)	180.0	0.003821	233.1	0.93	0.000131	188.7	0.99
Co(II)	163.0	0.001259	42.4	0.71	0.000124	181.8	0.99
Mn(II)	196.0	0.000825	19.6	0.41	0.00022	200.0	0.99

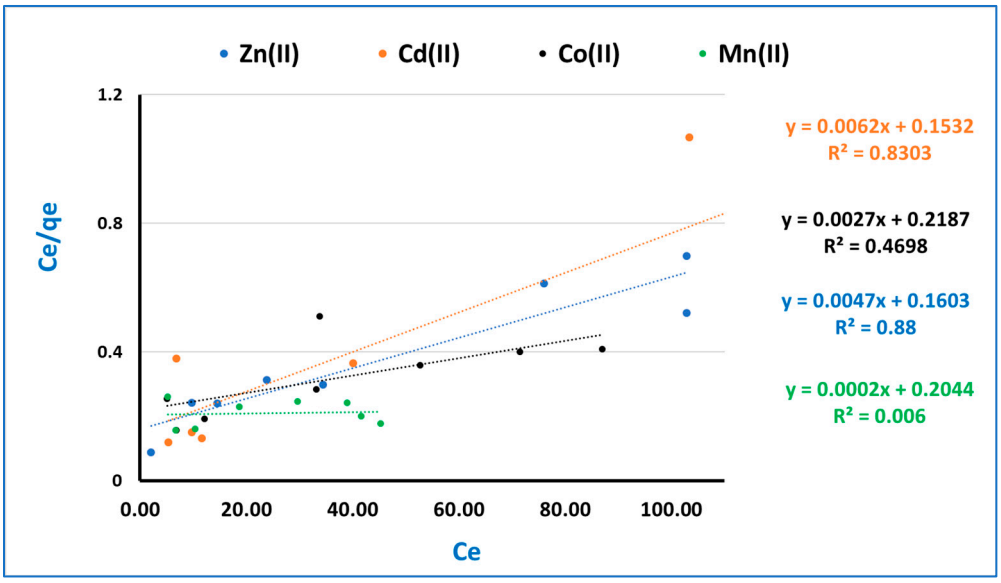

Figure 11. The Langmuir plot for adsorption of Zn(II), Cd(II), Co(II), and Mn(II) onto ZnO-C (pH: 6, 25 °C, and co. time: 180 min).

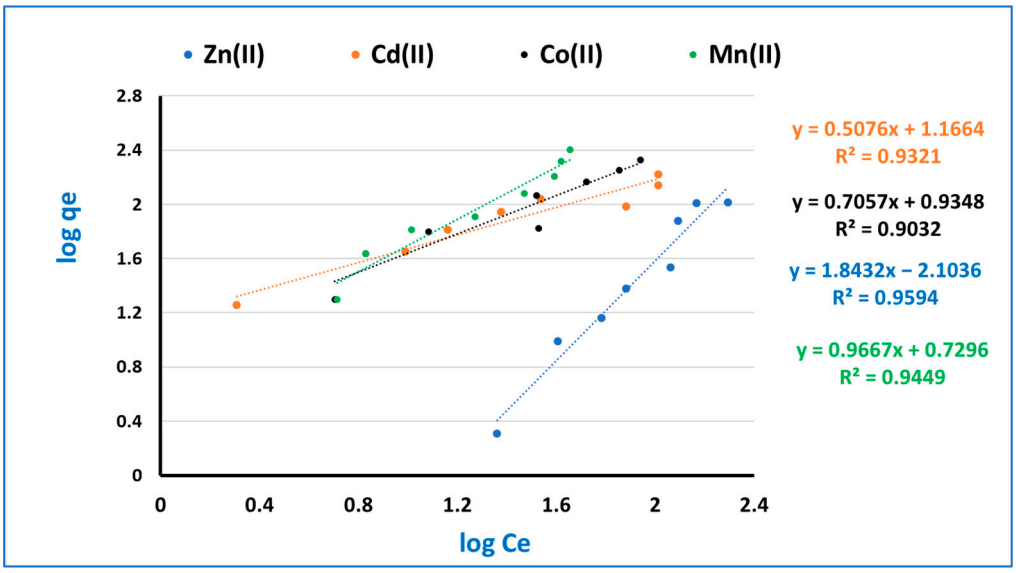

Figure 12. The Freundlich plot for adsorption of Zn(II), Cd(II), Co(II), and Mn(II) onto ZnO-C (pH: 6, 25 °C, and contact time: 180 min).

Table 4. Equilibrium isotherm constants for adsorption of Zn(II), Cd(II), Co(II), and Mn(II) onto ZnO-C.

Adsorbate (Heavy Metal Ion)	Langmuir Constant			Freundlich Constant		
	K_L	Q^0_{max}	R^2	K_F	n	R^2
Zn(II)	0.029	212.8	0.88	3.21	0.54	0.95
Cd(II)	0.040	161.3	0.83	2.55	1.97	0.93
Co(II)	0.012	370.4	0.46	2.55	1.42	0.90
Mn(II)	0.001	5000.0	0.006	2.07	1.03	0.94

3.5. Purification of Wastewater Using Deviled Hybrid Adsorbent Materials

As a result of environmental pollution, various water resources have been contaminated with toxic metals. In order to reduce the negative impacts of these heavy metals, the treatment of effluents with a high contaminate ratio is applied prior to them reaching natural water systems [58,59]. Various wastewater samples were brought from Riyadh City, Saudi Arabia. The developed adsorption process utilized ZnO-C and Fe_3O_4-C for the adsorption of Zn(II), Cd(II), Co(II), and Mn(II) from a real wastewater matrix (Table 5). The removal efficiency was not less than 91% for the tested samples. This level of the achieved adsorptive removal performance confirmed that the developed hybrid materials were effective for wastewater treatment in real field situations, with a high added value. By comparing the obtained results with results in the literature [60–81] (Table 6), it was observed that most of the applied materials exhibited the maximum adsorption capacity in a low-acidic medium and in a neutral medium. In addition, the performance efficiency of the evaluated hybrid martials in this work, including ZnO-C and Fe_3O_4, was superior compared to that of most of the tabulated adsorbents from the literature. However, a few adsorbent materials exhibited a higher adsorption capacity, such as ZnO nanoparticles [68], a hydroxyapatite/pectin hybrid material [78], and a zinc oxide/graphene oxide composite (ZnO/GO) [81].

Table 5. Utilization of ZnO-C and Fe_3O_4-C hybrid materials for real wastewater purification.

Adsorbent	Wastewater	Initial Concentration before Treatment (mg/L)				Detected Concentration after Treatment (mg/L)				Removal Efficiency %			
		Mn	Co	Cd	Zn	Mn	Co	Cd	Zn	Mn	Co	Cd	Zn
Carbon–Fe_3O_4	Valley Water	3.56	5.85	4.16	8.81	0.14	0.11	0.23	0.21	96	98	95	98
	Industrial Wastewater	15.64	21.04	17.04	11.81	0.43	1.40	1.14	0.79	97	93	93	93
	Rain Wastewater	1.50	2.51	1.91	3.43	0.06	0.00	0.08	0.30	96	100	96	91
Carbon–ZnO	Valley Water	3.56	5.85	4.16	8.81	0.05	0.18	0.10	0.14	99	97	98	98
	Industrial Wastewater	15.64	21.04	17.04	11.81	1.05	0.08	0.09	1.07	93	100	99	91
	Rain Wastewater	1.50	2.51	1.91	3.43	0.06	0.05	0.01	0.11	96	98	99	97

Table 6. Comparison of the adsorption performance of the ZnO-C and Fe_3O_4-C hybrid materials with materials from the literature.

Adsorbent	Adsorbate	Optimum	q_e	Ref.
Acid modified carbon-based adsorbents	Cd(II) ion	pH = 7 Contact time = 120 min	M-CNTs = 2.02 mg/g M-AC = 1.98 mg/g M-CNFs = 1.58 mg/g M-FA = 1.22 mg/g	[60]
Alumina coated multi-walled carbon nanotubes (MWCNTs)	Cd(II) ion trichloroethylene (TCE)	pH = 7 Contact time = 240 min	Cd(II) ion = 27.21 mg/g TCE = 19.84 mg/g	[61]

Table 6. *Cont.*

Adsorbent	Adsorbate	Optimum	q_e	Ref.
Natural kaolinite clay	Pb(II), Cd(II), Ni(II), and Cu(II)	pH = 5.5–7 Contact time = 30 min	Pb = 2.35 mg/g Cd = 0.88 mg/g Ni = 0.90 mg/g Cu = 1.22 mg/g	[62]
Functionalized carbon nanotubes and magnetic biochar	Zn(II)	pH = 10 Contact time = 120 min	Functionalized CNT = 1.05 mg/g Magnetic biochar = 1.18 mg/g	[63]
Poly(acrylic acid) multi-walled carbon nanotubes (MWCNT-g-PAAs)	Co(II)	pH = 6 Contact time = 300 min	3.55×10^{-4} molg^{-1}	[64]
Natural and modified clay	Mn(II) Cd(II)	pH = 1–6 Contact time = 60 min	NT-25/Cd(II) = 11.2 mg/g NT-25/Mn(II) = 6.0 mg/g	[65]
Natural phosphate (NP)	Cd(II)	pH = 5	26 mg/g	[66]
Straw biochar (WSB) and acid treated wheat straw biochar (AWSB)	Cd(II)	pH = 6 Contact time = 5–180 min	WSB = 31.65 mg/g AWSB = 74.63 mg/g	[67]
ZnO nanoparticles	Zn(II) Cd(II) Hg(II)	pH = 5.5	357 mg/g for Zn(II) 387 mg/g for Cd(II) 714 mg/g for Hg(II)	[68]
TiO_2 nanoparticles	Pb, Cd, Cu, Ni, Zn	pH = 8	-	[69]
Sugarcane leaves (SCLs)	Ni^{2+} Cr^{3+} Co^{2+}	pH = 8 for Cr^{3+}	51.3 mg/g for Ni^{2+} 62.5 mg/g for Cr^{3+} 66.7 mg/g for Co^{2+}	[70]
Graphene oxide bovine serum albumin (GO-BSA)	Co(II)	pH = 6	184 mg/g	[71]
Activated Saudi clays	Co(II)	-	12.9 mg/g for treated Tabbuk clay; 12.55 mg/g for treated Bahhah clay	[72]
Intact and modified Ficus carica leaves (FCLs)	Co(II)	pH = 6	33.9 mg/g	[73]
Polyaniline/sawdust composite	Mn(II)	pH = 10 Contact time = 30 min	58.824 mg/g	[74]
Poly(sodium acrylate) graphene oxide (PSA-GO) double network hydrogel	Mn(II) Cd(II)	pH = 6	Mn(II) = 165.5 mg/g Cd(II) = 238.3 mg/g	[75]
Surfactant modified alumina (SMA)	Mn(II)	pH = 4.04–8.05 Contact time = 30 min	2.04 mg/g	[76]
Activated carbon from bean pod waste	Mn(II) As(III)	pH = 5–6 Contact time = 30 min	Mn(II) = 23.4 mg/g As(III) = 1.01 mg/g	[77]
Hydroxyapatite/pectin hybrid material	Zn(II)	pH = 5	330.4 mg/g	[78]
Polyaniline nanocomposite coated on rice husk (PAn/RH)	Zn(II)	pH = 3 Contact time = 20 min	24.3 mg/g	[79]
Dendrimer conjugated magnetic nanoparticles	Zn(II)	pH = 7	24.3 mg/g	[80]
Zinc oxide nanoparticles (ZnO-NPs)	Cr^{3+}	pH = 3–7 Contact time = 20 min	88.547 mg/g	[32]

Table 6. *Cont.*

Adsorbent	Adsorbate	Optimum	q_e	Ref.
Zinc oxide/graphene oxide composite (ZnO/GO)	Pb(II)	pH = 5 Contact time = 160 min	909.09 mg/g	[81]
ZnO-C	Zn(II), Cd(II), Co(II), Mn(II)	pH = 6 Contact time = 180 min	Mn(II) = 196, Co(II) = 173, Cd(II) = 180, Zn(II) = 189 mg/g	This work
Fe_3O_4-C	Zn(II), Cd(II), Co(II), Mn(II)	pH = 6 Contact time = 180 min	Mn(II) = 167, Co(II) = 165, Cd(II) = 173, Zn(II) = 177 mg/g	This work

3.6. Regeneration Study for ZnO-C Recycling

Recycling the adsorbent materials serves environmental safety and supports the cost-effective wastewater treatment [82,83]. The fabricated ZnO-C hybrid adsorbent martials is investigated for multi-usage by regenerating it with a Na_2EDTA solution. The ZnO-C exhibited high reuse efficiency for adsorption of Zn(II), Cd(II), Co(II), and Mn(II). As presented in Figure 13, after four usage, the recycling efficiency is above 90%. These results reveal that the effectiveness of ZnO-C for sustainable applications as eco-friendly adsorbents.

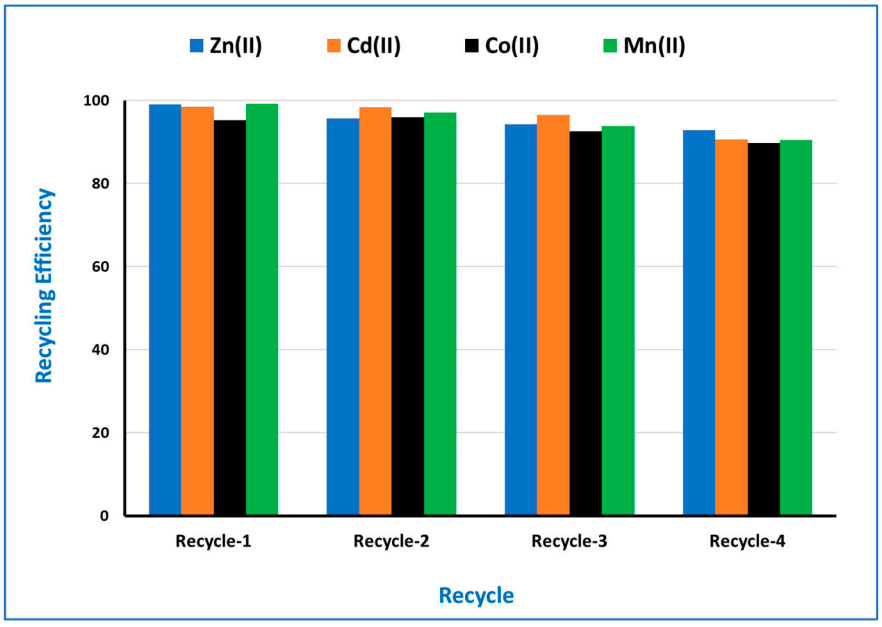

Figure 13. Recycling investigations for reuse of ZnO-C.

4. Conclusions

Zinc oxide nanoparticle anchored carbon (ZnO-C) hybrid adsorbent materials were prepared with a sphere-like granulated structure in the nanoscale size range of 16–68 nm. The EDS analysis indicated the presence of Zn on the granules' surfaces, together with carbon matric and oxygen. The prepared structure of ZnO-C had a surface area of 24.84 m^2/g. The optimized conditions for Zn(II), Cd(II), Co(II), and Mn(II) uptake were at a pH between 5 and 6, a contact time of 180 min, and a ZnO-C dose of 0.1 g/L. Real wastewater samples, including valley water, industrial wastewater, and rain water, were successfully treated through the adsorption of Zn(II), Cd(II), Co(II), and Mn(II) onto ZnO-C, indicating a high removal efficiency (more than 91%) for the evaluated samples. The results achieved in

this work suggest the need for further investigations to develop novel transition-metal-oxide-nanoparticle-coated carbon as a hybrid adsorbent material for enhanced wastewater treatment applications. In addition, the developed ZnO-C materials in this work could be investigated for additional applications, such as the photocatalytic degradation of organic pollutants and/or the removal of various pollutant categories such as radioactive waste and greenhouse gases.

Supplementary Materials: The following supporting information about instrumental analysis can be downloaded at: https://www.mdpi.com/article/10.3390/cryst14050447/s1.

Author Contributions: Conceptualization, M.A.H. and Z.A.A.; Formal analysis, M.A.H., Z.A.A. and A.-Y.B.-H.-A.; Investigation, A.G.A., M.A.H. and A.-Y.B.-H.-A.; Methodology, A.G.A., M.A.H. and A.-Y.B.-H.-A.; Resources, Z.A.A.; Supervision, Z.A.A. and A.-Y.B.-H.-A.; Validation, M.A.H., Z.A.A. and A.-Y.B.-H.-A.; Writing—original draft, A.G.A.; Writing—review and editing, M.A.H. and A.-Y.B.-H.-A. All authors have read and agreed to the published version of the manuscript.

Funding: This project was funded by the National Plan for Science, Technology, and Innovation (MAARIFAH), King Abdul Aziz City for Science and Technology, Kingdom of Saudi Arabia, award No. 13-ENV1186-02.

Data Availability Statement: The original contributions presented in the study are included in the article/Supplementary Materials, further inquiries can be directed to the corresponding author.

Acknowledgments: The author acknowledges the National Plan for Science, Technology, and Innovation (MAARIFAH), King Abdulaziz City for Science and Technology, Kingdom of Saudi Arabia for its grant with award number 13-ENV1186-02.

Conflicts of Interest: The authors declare no conflicts of interest.

References

1. Khalafi, T.; Buazar, F.; Ghanemi, K. Phycosynthesis and Enhanced Photocatalytic Activity of Zinc Oxide Nanoparticles Toward Organosulfur Pollutants. *Sci. Rep.* **2019**, *9*, 6866. [CrossRef] [PubMed]
2. Rengaraj, S.; Yeon, K.H.; Moon, S.H. Removal of Chromium from Water and Wastewater by Ion Exchange Resins. *J. Hazard. Mater.* **2001**, *87*, 273–287. [CrossRef] [PubMed]
3. Kurniawan, T.A.; Chan, G.Y.S.; Lo, W.; Babel, S. Comparisons of Low-Cost Adsorbents for Treating Wastewaters Laden with Heavy Metals. *Sci. Total Environ.* **2006**, *366*, 409–426. [CrossRef] [PubMed]
4. Weatherley, L.R.; Miladinovic, N.D. Comparison of the Ion Exchange Uptake of Ammonium Ion onto New Zealand Clinoptilolite and Mordenite. *Water Res.* **2004**, *38*, 4305–4312. [CrossRef] [PubMed]
5. Ljung, K.; Vahter, M. Time to Re-Evaluate the Guideline Value for Manganese in Drinking Water? *Environ. Health Perspect.* **2007**, *115*, 1533–1538. [CrossRef] [PubMed]
6. Agusa, T.; Kunito, T.; Fujihara, J.; Kubota, R.; Minh, T.B.; Kim Trang, P.T.; Iwata, H.; Subramanian, A.; Viet, P.H.; Tanabe, S. Contamination by Arsenic and Other Trace Elements in Tube-Well Water and Its Risk Assessment to Humans in Hanoi, Vietnam. *Environ. Pollut.* **2006**, *139*, 95–106. [CrossRef]
7. Griffin, A.E. Significance and Removal of Manganese in Water Supplies. *J. Am. Water Works Assoc.* **1960**, *52*, 1326–1334. [CrossRef]
8. Sankhla, M.S.; Kumar, R.; Prasad, L. Zinc Impurity in Drinking Water and Its Toxic Effect on Human Health. *Indian Internet J. Forensic Med. Toxicol.* **2019**, *17*, 84. [CrossRef]
9. Sankhla, M.S.; Kumar, R. Contaminant of Heavy Metals in Groundwater & Its Toxic Effects on Human Health & Environment. *Int. J. Environ. Sci. Nat. Resour.* **2019**, *18*, 1–5. [CrossRef]
10. Porea, T.J.; Belmont, J.W.; Maboney, D.H. Zinc-Induced Anemia and Neutropenia in an Adolescent. *J. Pediatr.* **2000**, *136*, 688–690. [CrossRef]
11. Nogawa, K.; Kobayashi, E.; Okubo, Y.; Suwazono, Y. Environmental Cadmium Exposure, Adverse Effects and Preventive Measures in Japan. *BioMetals* **2004**, *17*, 581–587. [CrossRef] [PubMed]
12. Chand, P. Environmental Protection and Regulations in India: Role of the Central Pollution Control Board. *Indian J. Public Adm.* **2018**, *64*, 645–663. [CrossRef]
13. Gupta, V.K.; Gupta, M.; Sharma, S. Process Development for the Removal of Lead and Chromium from Aqueous Solutions Using Red Mud—An Aluminium Industry Waste. *Water Res.* **2001**, *35*, 1125–1134. [CrossRef] [PubMed]
14. Dubey, A.; Shiwani, S. Adsorption of Lead Using a New Green Material Obtained from Portulaca Plant. *Int. J. Environ. Sci. Technol.* **2012**, *9*, 15–20. [CrossRef]
15. Järup, L. Hazards of Heavy Metal Contamination. *Br. Med. Bull.* **2003**, *68*, 167–182. [CrossRef]
16. Esalah, J.O.; Weber, M.E.; Vera, J.H. Removal of Lead, Cadmium and Zinc from Aqueous Solutions by Precipitation with Sodium Di-(n-Octyl) Phosphinate. *Can. J. Chem. Eng.* **2000**, *78*, 948–954. [CrossRef]

17. Inyang, M.; Gao, B.; Yao, Y.; Xue, Y.; Zimmerman, A.R.; Pullammanappallil, P.; Cao, X. Removal of Heavy Metals from Aqueous Solution by Biochars Derived from Anaerobically Digested Biomass. *Bioresour. Technol.* **2012**, *110*, 50–56. [CrossRef]
18. Sigdel, A.; Jung, W.; Min, B.; Lee, M.; Choi, U.; Timmes, T.; Kim, S.J.; Kang, C.U.; Kumar, R.; Jeon, B.H. Concurrent Removal of Cadmium and Benzene from Aqueous Solution by Powdered Activated Carbon Impregnated Alginate Beads. *CATENA* **2017**, *148*, 101–107. [CrossRef]
19. Chen, L.; Wu, P.; Chen, M.; Lai, X.; Ahmed, Z.; Zhu, N.; Dang, Z.; Bi, Y.; Liu, T. Preparation and Characterization of the Eco-Friendly Chitosan/Vermiculite Biocomposite with Excellent Removal Capacity for Cadmium and Lead. *Appl. Clay Sci.* **2018**, *159*, 74–82. [CrossRef]
20. Elhafez, S.E.A.; Hamad, H.A.; Zaatout, A.A.; Malash, G.F. Management of Agricultural Waste for Removal of Heavy Metals from Aqueous Solution: Adsorption Behaviors, Adsorption Mechanisms, Environmental Protection, and Techno-Economic Analysis. *Environ. Sci. Pollut. Res.* **2017**, *24*, 1397–1415. [CrossRef]
21. Bouhamed, F.; Elouear, Z.; Bouzid, J.; Ouddane, B. Multi-Component Adsorption of Copper, Nickel and Zinc from Aqueous Solutions onto Activated Carbon Prepared from Date Stones. *Environ. Sci. Pollut. Res.* **2016**, *23*, 15801–15806. [CrossRef] [PubMed]
22. Lehmann, J. A handful of carbon. *Nature* **2007**, *447*, 143–144. [CrossRef] [PubMed]
23. Makhesana, M.A.; Patel, K.M.; Nyabadza, A. Applicability of Nanomaterials in Water and Waste-Water Treatment: A State-of-the-Art Review and Future Perspectives. *Mater. Today Proc.* **2024**. [CrossRef]
24. Habila, M.A.; Alothman, Z.A.; El-Toni, A.M.; Al-Tamrah, S.A.; Soylak, M.; Labis, J.P. Carbon-Coated Fe_3O_4 Nanoparticles with Surface Amido Groups for Magnetic Solid Phase Extraction of Cr(III), Co(II), Cd(II), Zn(II) and Pb(II) Prior to Their Quantitation by ICP-MS. *Microchim. Acta* **2017**, *184*, 2645–2651. [CrossRef]
25. Raveendran, P.; Fu, J.; Wallen, S.L. Completely "Green" Synthesis and Stabilization of Metal Nanoparticles. *J. Am. Chem. Soc.* **2003**, *125*, 13940–13941. [CrossRef] [PubMed]
26. Fernandes, D.M.; Silva, R.; Hechenleitner, A.A.W.; Radovanovic, E.; Melo, M.A.C.; Pineda, E.A.G. Synthesis and Characterization of ZnO, CuO and a Mixed Zn and Cu Oxide. *Mater. Chem. Phys.* **2009**, *115*, 110–115. [CrossRef]
27. Buazar, F.; Bavi, M.; Kroushawi, F.; Halvani, M.; Khaledi-Nasab, A.; Hossieni, S.A. Potato Extract as Reducing Agent and Stabiliser in a Facile Green One-Step Synthesis of ZnO Nanoparticles. *J. Exp. Nanosci.* **2016**, *11*, 175–184. [CrossRef]
28. Hoffman, R.L. ZnO Thin-Film Transistors. In *Zinc Oxide Bulk, Thin Films and Nanostructures: Processing, Properties and Applications*; Elsevier Science Ltd.: Amsterdam, The Netherlands, 2006; pp. 415–442. [CrossRef]
29. Kolodziejczak-Radzimska, A.; Jesionowski, T. Zinc Oxide-from Synthesis to Application: A Review. *Materials* **2014**, *7*, 2833–2881. [CrossRef]
30. Kamath, S.; Gopal, V.; Ramanjaneyalu, V.; Kamila, S. Application of ZnO Nano Rods for the Batch Adsorption of Cr(VI): A Study of Kinetics and Isotherms. *Am. J. Appl. Sci.* **2019**, *16*, 101–112. [CrossRef]
31. Al-Mur, B.A. Green Zinc Oxide (ZnO) Nanoparticle Synthesis Using Mangrove Leaf Extract from Avicenna Marina: Properties and Application for the Removal of Toxic Metal Ions (Cd2+ and Pb2+). *Water* **2023**, *15*, 455. [CrossRef]
32. Gu, M.; Hao, L.; Wang, Y.; Li, X.; Chen, Y.; Li, W.; Jiang, L. The Selective Heavy Metal Ions Adsorption of Zinc Oxide Nanoparticles from Dental Wastewater. *Chem. Phys.* **2020**, *534*, 110750. [CrossRef]
33. Dhiman, V.; Kondal, N. ZnO Nanoadsorbents: A Potent Material for Removal of Heavy Metal Ions from Wastewater. *Colloid Interface Sci. Commun.* **2021**, *41*, 100380. [CrossRef]
34. Buazar, F.; Alipouryan, S.; Kroushawi, F.; Hossieni, S.A. Photodegradation of Odorous 2-Mercaptobenzoxazole through Zinc Oxide/Hydroxyapatite Nanocomposite. *Appl. Nanosci.* **2015**, *5*, 719–729. [CrossRef]
35. Arularasu, M.V.; Sendhil, M.; Rajendran, T.V.; Mani, G.; Aljuwayid, A.M.; Habila, M.A. Recent Advantages of Zinc Oxide/Carbon Nanotubes/Reduced Graphene Oxide Based Nanocomposite for the Visible Light Photodegradation. *Inorg. Chem. Commun.* **2022**, *139*, 109332. [CrossRef]
36. Oyewo, O.A.; Adeniyi, A.; Sithole, B.B.; Onyango, M.S. Sawdust-Based Cellulose Nanocrystals Incorporated with ZnO Nanoparticles as Efficient Adsorption Media in the Removal of Methylene Blue Dye. *ACS Omega* **2020**, *5*, 18798–18807. [CrossRef]
37. Liu, C.; Qian, X.; Wei, Q.; Chen, Z.; Chen, J.; Wang, W.; Chen, X.; Gao, J.; Liu, Y.; Xie, L. Construction of Hydrostable Cesium Lead Bromide-Titania for Visible-Light Degradation of Tetracycline Hydrochloride in Water. *J. Clean. Prod.* **2022**, *365*, 132830. [CrossRef]
38. He, H.; Wang, X.; Yu, Q.; Wu, W.; Feng, X.; Kong, D.; Ren, X.; Gao, J. In Situ Growth of Ti3C2/UiO-66-NH2 Composites for Photoreduction of Cr(VI). *Catalysts* **2023**, *13*, 876. [CrossRef]
39. Nie, D.; Wang, P.; Zang, C.; Zhang, G.; Li, S.; Liu, R.; Zhang, Y.; Li, G.; Luo, Y.; Zhang, W.; et al. Preparation of ZnO-Incorporated Porous Carbon Nanofibers and Adsorption Performance Investigation on Methylene Blue. *ACS Omega* **2022**, *7*, 2198–2204. [CrossRef] [PubMed]
40. Durmus, Z.; Kurt, B.Z.; Durmus, A. Synthesis and Characterization of Graphene Oxide/Zinc Oxide (GO/ZnO) Nanocomposite and Its Utilization for Photocatalytic Degradation of Basic Fuchsin Dye. *ChemistrySelect* **2019**, *4*, 271–278. [CrossRef]
41. Ali, Q.; Zia, M.A.; Kamran, M.; Shabaan, M.; Zulfiqar, U.; Ahmad, M.; Iqbal, R.; Maqsood, M.F. Nanoremediation for Heavy Metal Contamination: A Review. *Hybrid Adv.* **2023**, *4*, 100091. [CrossRef]
42. Ethaib, S.; Al-Qutaifia, S.; Al-Ansari, N.; Zubaidi, S.L. Function of Nanomaterials in Removing Heavy Metals for Water and Wastewater Remediation: A Review. *Environments* **2022**, *9*, 123. [CrossRef]

43. S, D.S.; Vishwakarma, V. Recovery and Recycle of Wastewater Contaminated with Heavy Metals Using Adsorbents Incorporated from Waste Resources and Nanomaterials—A Review. *Chemosphere* **2021**, *273*, 129677. [CrossRef] [PubMed]
44. Habila, M.A.; Moshab, M.S.; El-Toni, A.M.; ALOthman, Z.A.; Badjah Hadj Ahmed, A.Y. Thermal Fabrication of Magnetic Fe3O4 (Nanoparticle)@Carbon Sheets from Waste Resources for the Adsorption of Dyes: Kinetic, Equilibrium, and UV–Visible Spectroscopy Investigations. *Nanomaterials* **2023**, *13*, 1266. [CrossRef] [PubMed]
45. Habila, M.A.; Sheikh Moshab, M.; Mohamed El-Toni, A.; Al-Awadi, A.S.; ALOthman, Z.A. Facile Strategy for Fabricating an Organosilica-Modified Fe_3O_4 (OS/Fe_3O_4) Hetero-Nanocore and OS/Fe3O4@SiO2 Core–Shell Structure for Wastewater Treatment with Promising Recyclable Efficiency. *ACS Omega* **2023**, *8*, 7626–7638. [CrossRef] [PubMed]
46. Fouladi-Fard, R.; Aali, R.; Mohammadi-Aghdam, S.; Mortazavi-derazkola, S. The Surface Modification of Spherical ZnO with Ag Nanoparticles: A Novel Agent, Biogenic Synthesis, Catalytic and Antibacterial Activities. *Arab. J. Chem.* **2022**, *15*, 103658. [CrossRef]
47. Al-Rawashdeh, N.A.F.; Allabadi, O.; Aljarrah, M.T. Photocatalytic Activity of Graphene Oxide/Zinc Oxide Nanocomposites with Embedded Metal Nanoparticles for the Degradation of Organic Dyes. *ACS Omega* **2020**, *5*, 28046–28055. [CrossRef]
48. Pascariu, P.; Olaru, N.; Rotaru, A.; Airinei, A. Innovative Low-Cost Carbon/ZnO Hybrid Materials with Enhanced Photocatalytic Activity towards Organic Pollutant Dyes' Removal. *Nanomaterials* **2020**, *10*, 1873. [CrossRef]
49. Narjis, A.; El Aakib, H.; Boukendil, M.; El Hasnaoui, M.; Nkhaili, L.; Aberkouks, A.; Outzourhit, A. Controlling the Structural Properties of Pure and Aluminum Doped Zinc Oxide Nanoparticles by Annealing. *J. King Saud Univ. Sci.* **2020**, *32*, 1074–1080. [CrossRef]
50. Wu, R.; Bao, A. Preparation of Cellulose Carbon Material from Cow Dung and Its CO_2 Adsorption Performance. *J. CO2 Util.* **2023**, *68*, 102377. [CrossRef]
51. Van Hung, N.; Nguyet, B.T.M.; Nghi, N.H.; Khieu, D.Q. Photocatalytic Degradation of Methylene Blue by Using ZnO/Longan Seed Activated Carbon Under Visible-Light Region. *J. Inorg. Organomet. Polym. Mater.* **2021**, *31*, 446–459. [CrossRef]
52. Rodríguez, C.; Tapia, C.; Leiva-Aravena, E.; Leiva, E. Graphene Oxide–ZnO Nanocomposites for Removal of Aluminum and Copper Ions from Acid Mine Drainage Wastewater. *Int. J. Environ. Res. Public Health* **2020**, *17*, 6911. [CrossRef] [PubMed]
53. Hadadian, M.; Goharshadi, E.K.; Fard, M.M.; Ahmadzadeh, H.; Hadadian, M.; Goharshadi, E.K.; Fard, M.M.; Ahmadzadeh, H. Synergistic Effect of Graphene Nanosheets and Zinc Oxide Nanoparticles for Effective Adsorption of Ni (II) Ions from Aqueous Solutions. *ApPhA* **2018**, *124*, 239. [CrossRef]
54. Leiva, E.; Tapia, C.; Rodríguez, C.; Palet, C.; Bastos-Arrieta, J. Highly Efficient Removal of Cu(II) Ions from Acidic Aqueous Solution Using ZnO Nanoparticles as Nano-Adsorbents. *Water* **2021**, *13*, 2960. [CrossRef]
55. Habila, M.A.; ALOthman, Z.A.; Hakami, H.M.; Alanazi, A.G. Influence of Synthesis-Heating Conditions on the Porosity and Performance of a Carbon Nanotube/SDS-Alumina Nanocomposite for Effective Wastewater Treatment: Fabrication, Characterization, and Adsorption Modeling. *Ind. Eng. Chem. Res.* **2023**, *62*, 12571–12588. [CrossRef]
56. Habila, M.A.; ALOthman, Z.A.; Hakami, H.M.; ALOthman, M.R.; Sheikh, M. Recyclable Carbon-Based Hybrid Adsorbents Functionalized with Alumina Nanoparticles for Water Remediation. *Crystals* **2023**, *13*, 598. [CrossRef]
57. Mohamed El-Toni, A.; Habila, M.A.; Abbas Ibrahim, M.; Puzon Labis, J.; ALOthman, Z.A. Simple and Facile Synthesis of Amino Functionalized Hollow Core–Mesoporous Shell Silica Spheres Using Anionic Surfactant for Pb (II), Cd (II), and Zn (II) Adsorption and Recovery. *Chem. Eng. J.* **2014**, *251*, 441–451. [CrossRef]
58. Chen, L.; Hu, N.; Zhao, C.; Sun, X.; Han, R.; Lv, Y.; Zhang, Z. High-Efficiency Foam Fractionation of Anthocyanin from Perilla Leaves Using Surfactant-Free Active Al2O3 Nanoparticle as Collector and Frother: Performance and Mechanism. *Food Chem.* **2023**, *427*, 136708. [CrossRef] [PubMed]
59. Burakov, A.E.; Galunin, E.V.; Burakova, I.V.; Kucherova, A.E.; Agarwal, S.; Tkachev, A.G.; Gupta, V.K. Adsorption of Heavy Metals on Conventional and Nanostructured Materials for Wastewater Treatment Purposes: A Review. *Ecotoxicol. Environ. Saf.* **2018**, *148*, 702–712. [CrossRef]
60. Ihsanullah; Al-Khaldi, F.A.; Abusharkh, B.; Khaled, M.; Atieh, M.A.; Nasser, M.S.; Laoui, T.; Saleh, T.A.; Agarwal, S.; Tyagi, I.; et al. Adsorptive Removal of Cadmium(II) Ions from Liquid Phase Using Acid Modified Carbon-Based Adsorbents. *J. Mol. Liq.* **2015**, *204*, 255–263. [CrossRef]
61. Liang, J.; Liu, J.; Yuan, X.; Dong, H.; Zeng, G.; Wu, H.; Wang, H.; Liu, J.; Hua, S.; Zhang, S.; et al. Facile Synthesis of Alumina-Decorated Multi-Walled Carbon Nanotubes for Simultaneous Adsorption of Cadmium Ion and Trichloroethylene. *Chem. Eng. J.* **2015**, *273*, 101–110. [CrossRef]
62. Jiang, M.Q.; Jin, X.Y.; Lu, X.Q.; Chen, Z.L. Adsorption of Pb(II), Cd(II), Ni(II) and Cu(II) onto Natural Kaolinite Clay. *Desalination* **2010**, *252*, 33–39. [CrossRef]
63. Mubarak, N.M.; Alicia, R.F.; Abdullah, E.C.; Sahu, J.N.; Haslija, A.B.A.; Tan, J. Statistical Optimization and Kinetic Studies on Removal of Zn2+ Using Functionalized Carbon Nanotubes and Magnetic Biochar. *J. Environ. Chem. Eng.* **2013**, *1*, 486–495. [CrossRef]
64. Chen, H.; Li, J.; Shao, D.; Ren, X.; Wang, X. Poly(Acrylic Acid) Grafted Multiwall Carbon Nanotubes by Plasma Techniques for Co(II) Removal from Aqueous Solution. *Chem. Eng. J.* **2012**, *210*, 475–481. [CrossRef]
65. Dal Bosco, S.M.; Jimenez, R.S.; Vignado, C.; Fontana, J.; Geraldo, B.; Figueiredo, F.C.A.; Mandelli, D.; Carvalho, W.A. Removal of Mn(II) and Cd(II) from Wastewaters by Natural and Modified Clays. *Adsorption* **2006**, *12*, 133–146. [CrossRef]

66. Yaacoubi, H.; Zidani, O.; Mouflih, M.; Gourai, M.; Sebti, S. Removal of Cadmium from Water Using Natural Phosphate as Adsorbent. *Procedia Eng.* **2014**, *83*, 386–393. [CrossRef]
67. Naeem, M.A.; Imran, M.; Amjad, M.; Abbas, G.; Tahir, M.; Murtaza, B.; Zakir, A.; Shahid, M.; Bulgariu, L.; Ahmad, I. Batch and Column Scale Removal of Cadmium from Water Using Raw and Acid Activated Wheat Straw Biochar. *Water* **2019**, *11*, 1438. [CrossRef]
68. Sheela, T.; Nayaka, Y.A.; Viswanatha, R.; Basavanna, S.; Venkatesha, T.G. Kinetics and Thermodynamics Studies on the Adsorption of Zn(II), Cd(II) and Hg(II) from Aqueous Solution Using Zinc Oxide Nanoparticles. *Powder Technol.* **2012**, *217*, 163–170. [CrossRef]
69. Engates, K.E.; Shipley, H.J. Adsorption of Pb, Cd, Cu, Zn, and Ni to Titanium Dioxide Nanoparticles: Effect of Particle Size, Solid Concentration, and Exhaustion. *Environ. Sci. Pollut. Res.* **2011**, *18*, 386–395. [CrossRef] [PubMed]
70. Adigun, O.A.; Oninla, V.O.; Babarinde, N.A.A.; Oyedotun, K.O.; Manyala, N. Characterization of Sugarcane Leaf-Biomass and Investigation of Its Efficiency in Removing Nickel(II), Chromium(III) and Cobalt(II) Ions from Polluted Water. *Surf. Interfaces* **2020**, *20*, 100621. [CrossRef]
71. Joshi, S.; Singh, H.; Sharma, S.; Barman, P.; Saini, A.; Verma, G. Synthesis and Characterization of Graphene Oxide-Bovine Serum Albumin Conjugate Membrane for Adsorptive Removal of Cobalt(II) from Water. *Int. J. Environ. Sci. Technol.* **2021**, *18*, 3915–3928. [CrossRef]
72. Al-Jlil, S.A. Adsorption of Cobalt Ions from Waste Water on Activated Saudi Clays. *Appl. Water Sci.* **2017**, *7*, 383–391. [CrossRef]
73. Dabbagh, R.; Ashtiani Moghaddam, Z.; Ghafourian, H. Removal of Cobalt(II) Ion from Water by Adsorption Using Intact and Modified Ficus Carica Leaves as Low-Cost Natural Sorbent. *Desalination Water Treat.* **2016**, *57*, 19890–19902. [CrossRef]
74. Qomi, M.H.; Eisazadeh, H.; Hosseini, M.; Namaghi, H.A. Manganese Removal from Aqueous Media Using Polyaniline Nanocomposite Coated on Wood Sawdust. *Synth. Met.* **2014**, *194*, 153–159. [CrossRef]
75. Xu, R.; Zhou, G.; Tang, Y.; Chu, L.; Liu, C.; Zeng, Z.; Luo, S. New Double Network Hydrogel Adsorbent: Highly Efficient Removal of Cd(II) and Mn(II) Ions in Aqueous Solution. *Chem. Eng. J.* **2015**, *275*, 179–188. [CrossRef]
76. Khobragade, M.U.; Pal, A. Investigation on the Adsorption of Mn(II) on Surfactant-Modified Alumina: Batch and Column Studies. *J. Environ. Chem. Eng.* **2014**, *2*, 2295–2305. [CrossRef]
77. Budinova, T.; Savova, D.; Tsyntsarski, B.; Ania, C.O.; Cabal, B.; Parra, J.B.; Petrov, N. Biomass Waste-Derived Activated Carbon for the Removal of Arsenic and Manganese Ions from Aqueous Solutions. *Appl. Surf. Sci.* **2009**, *255*, 4650–4657. [CrossRef]
78. Ni, P.; Fox, J.T. Synthesis and Appraisal of a Hydroxyapatite/Pectin Hybrid Material for Zinc Removal from Water. *RSC Adv.* **2019**, *9*, 21095–21105. [CrossRef] [PubMed]
79. Ghorbani, M. Removal of Zinc Ions from Aqueous Solution Using Polyaniline Nanocomposite Coated on Rice Husk. *Iran. J. Energy Environ.* **2012**, *3*, 66–71. [CrossRef]
80. Chou, C.M.; Lien, H.L. Dendrimer-Conjugated Magnetic Nanoparticles for Removal of Zinc (II) from Aqueous Solutions. *J. Nanopart. Res.* **2011**, *13*, 2099–2107. [CrossRef]
81. Ahmad, S.Z.N.; Salleh, W.N.W.; Yusof, N.; Mohd Yusop, M.Z.; Hamdan, R.; Awang, N.A.; Ismail, N.H.; Rosman, N.; Sazali, N.; Ismail, A.F. Pb(II) Removal and Its Adsorption from Aqueous Solution Using Zinc Oxide/Graphene Oxide Composite. *Chem. Eng. Commun.* **2021**, *208*, 646–660. [CrossRef]
82. Momina; Shahadat, M.; Isamil, S. Regeneration Performance of Clay-Based Adsorbents for the Removal of Industrial Dyes: A Review. *RSC Adv.* **2018**, *8*, 24571–24587. [CrossRef]
83. Dai, Y.; Zhang, N.; Xing, C.; Cui, Q.; Sun, Q. The Adsorption, Regeneration and Engineering Applications of Biochar for Removal Organic Pollutants: A Review. *Chemosphere* **2019**, *223*, 12–27. [CrossRef]